Automatica 52 (2015) 1–7

Contents lists available at ScienceDirect

Automatica

journal homepage: www.elsevier.com/locate/automatica

Brief paper

Control of VTOL vehicles with thrust-tilting augmentation☆

Minh-Duc Hua [a,1], Tarek Hamel [b], Pascal Morin [a], Claude Samson [c,b]

[a] ISIR UPMC-CNRS, Paris, France
[b] I3S UNSA-CRNS, Sophia-Antipolis, France
[c] INRIA, France

ARTICLE INFO

Article history:
Received 22 November 2013
Received in revised form
10 June 2014
Accepted 21 October 2014

Keywords:
Nonlinear control
Thrust-tilting VTOL vehicle
Hierarchical objectives

ABSTRACT

An approach to the control of a VTOL vehicle equipped with complementary thrust-tilting capabilities that nominally yield full actuation of the vehicle's position and attitude is developed. The particularity and difficulty of the control problem are epitomized by the existence of a maximum tilting angle which forbids complete and decoupled control of the vehicle's position and attitude in all situations. This problem is here addressed via the formalism of primary and secondary objectives and by extending a solution previously derived in the fixed thrust-direction case. The proposed control design is also illustrated by simulation results involving a quadrotor UAV with all propeller axes pointing in the same monitored tilted direction.

1. Introduction

A mechanical design and feedback control of small aerial vehicles possessing thrust vectoring capabilities have received an increasing interest in recent years and given rise to various declinations (Cetinsoy et al., 2012; Kendoul, Fantoni, & Lozano, 2005; Long & Cappelleri, 2013; Muraoka, Okada, & Kubo, 2009; Naldi, Marconi, & Sala, 2008; Notarstefano & Hauser, 2010; Papachristos, Alexis, & Tzes, 2011; Pflimlin, Binetti, Souères, Hamel, & Trouchet, 2010; Russo, Notarstefano, & Hauser, 2011; Ryll, Bulthoff, & Giordano, 2012). For instance, the concepts of twin tilt-rotors (Kendoul et al., 2005; Papachristos et al., 2011), tilt-wing UAVs (Cetinsoy et al., 2012; Muraoka et al., 2009), and quadrotor UAVs with two orthogonal tilting axes (Ryll et al., 2012) are worth mentioning. Thrust vectoring for an aerial vehicle is the ability to modify the direction of the propulsion thrust with respect to (w.r.t.) a body-fixed frame. This feature can be used either for attitude (i.e. orientation) control, when the thrust rotation center is located at some distance of the vehicle's center of mass (CoM) with thrust vectoring yielding torque creation, as in the case of rocket nozzle tilting or ducted-fan airflow derivation via the use of rotating surfaces (Naldi et al., 2008; Pflimlin et al., 2010), or for attitude/position control decoupling, when the thrust rotation center is near the CoM and complementary actuation for attitude control is available, as in the case of V/STOL aircraft whose fuselage orientation is controlled independently of the vehicle's longitudinal motion (Notarstefano & Hauser, 2010; Russo et al., 2011). In fact, thrust vectoring can also be used to achieve a combination of the aforementioned objectives. This multiple usage renders the term *thrust-vectoring* somewhat imprecise. We use here the term *thrust tilting* in reference to the second possibility, i.e. attitude and longitudinal motion control decoupling. In this case, thrust-direction tilting involves two actuated degrees of freedom (d.o.f.) which complement the conventional four actuated d.o.f. associated with common aerial vehicles, namely thrust intensity plus three torque components necessary for complete attitude control. This yields six independent actuated d.o.f. that allow for the complete control of the six-dimensional state. A similar objective is addressed in Ryll et al. (2012) where the vehicle under consideration is a quadrotor UAV, whose propeller axes rotate two by two about one of the two orthogonal axes of the quadrotor. The control design proposed in Ryll et al. (2012) basically relies on exact linearization of the vehicle's motion equations. This control strategy, combined with actuation redundancy, in turn leads to a control calculation based on the use of pseudo-inverse matrices and on solving a complementary optimization problem (e.g., energy

☆ This work was supported by the French Agence Nationale de la Recherche via the ANR ASTRID SCAR project "Sensory Control of Aerial Robots" (ANR-12-ASTR-0033) and via the ROBOTEX project (ANR-10-EQPX-44-01), and by the Chaire d'excellence en robotique RTE-UPMC "Mini-drones autonomes". The material in this paper was presented at the 19th IFAC World Congress, August 24–29, 2014, Cape Town, South Africa. This paper was recommended for publication in revised form by Associate Editor Abdelhamid Tayebi under the direction of Editor Toshiharu Sugie.

E-mail addresses: hua@isir.upmc.fr (M.-D. Hua), thamel@i3s.unice.fr (T. Hamel), morin@isir.upmc.fr (P. Morin), Claude.Samson@inria.fr, csamson@i3s.unice.fr (C. Samson).

[1] Tel.: +33 0 144276362.

http://dx.doi.org/10.1016/j.automatica.2014.10.129
0005-1098/

expenditure minimization). However, thrust-tilting angle limitations are not taken into account in that study.

With respect to Ryll et al. (2012), we here address thrust tilting in the form of a generic problem whose solution potentially applies to a large panel of aerial vehicles with extended flight envelopes. Such a claim of generality imposes to take aerodynamic forces acting on the vehicle into account. For control design purposes, simplified models of these forces are used. The proposed (nonlinear) control design is also different from that of Ryll et al. (2012). It is an extension of the one presented in Hua, Hamel, Morin, and Samson (2009, 2013) for reference velocity or position tracking in the case where the thrust direction is fixed, and it is based on a Lyapunov-like approach. An important original outcome of the present study is that vectoring limitations are taken into account explicitly. More precisely, it is assumed that the thrust-tilting angle w.r.t. a "neutral" direction, corresponding for instance to the one associated with the fixed direction of a conventional quadrotor UAV, cannot exceed a known threshold. Due to this limitation, independent control of the vehicle's attitude and position is no longer always possible. This leads naturally to set priorities between complementary control objectives. Accordingly, the proposed control methodology involves a *primary* objective associated with the reference velocity or position asymptotic stabilization, and a *secondary* objective associated with the asymptotic stabilization of a reference orientation for a body-fixed frame. Beside provable stability and convergence properties in a large domain of operation, we believe that the conceptual simplicity of the solution, the non-requirement of switching between several control laws, and the ability to monitor smoothly transition phases constitute to valuable complementary assets. Its geometric nature shows through its construction in the framework of affine geometry and its expression, mostly coordinates-free, also distinguishes it from linear and other nonlinear control methods employed in the domains of aeronautics and aerial robotics.

A primary version of this work has been presented at a conference (Hua, Hamel, Morin, & Samson, 2014).

2. Preliminary material

2.1. Notation

- $\boldsymbol{E}^3$ denotes the three-dimensional Euclidean vector space. Vectors in $\boldsymbol{E}^3$ are denoted with bold letters. Inner and cross products in $\boldsymbol{E}^3$ are denoted by the symbols $\cdot$ and $\times$, respectively. The i_{th} component of $x \in \mathbb{R}^n$ is denoted as x_i. Given $x = (x_1, x_2, x_3)^T \in \mathbb{R}^3$, for the sake of conciseness $(x_1\boldsymbol{\imath} + x_2\boldsymbol{\jmath} + x_3\boldsymbol{k})$ is written as $(\boldsymbol{\imath}, \boldsymbol{\jmath}, \boldsymbol{k})x$, and $x_{1,2}$ denotes the vector of first two components of x.
- $\mathcal{I} = \{O; \boldsymbol{\imath_0}, \boldsymbol{\jmath_0}, \boldsymbol{k_0}\}$ and $\mathcal{B} = \{G; \boldsymbol{\imath}, \boldsymbol{\jmath}, \boldsymbol{k}\}$, with G the vehicle's center of mass (CoM), denote the inertial frame and body-fixed frame, respectively.
- $\boldsymbol{T} = -T\boldsymbol{u}$ denotes the thrust force, with the minus sign arising from a convention used for VTOL vehicles and $\boldsymbol{u}$ the unit vector of the thrust axis.
- u and $\dot{u}$ denote the vector of coordinates, on the basis of $\mathcal{B}$, of $\boldsymbol{u}$ and $\frac{d}{dt}\boldsymbol{u}_{|\mathcal{B}}$, respectively, i.e. $\boldsymbol{u} = (\boldsymbol{\imath}, \boldsymbol{\jmath}, \boldsymbol{k})u$ and $\frac{d}{dt}\boldsymbol{u}_{|\mathcal{B}} = (\boldsymbol{\imath}, \boldsymbol{\jmath}, \boldsymbol{k})\dot{u}$.
- $\boldsymbol{\omega}^u_{\mathcal{I}} = \boldsymbol{u} \times \frac{d}{dt}\boldsymbol{u}_{|\mathcal{I}}$ and $\boldsymbol{\omega}^u_{\mathcal{B}} = \boldsymbol{u} \times \frac{d}{dt}\boldsymbol{u}_{|\mathcal{B}}$ denote the angular velocity of $\boldsymbol{u}$ w.r.t. the inertial frame and the body-fixed frame, respectively.
- $\boldsymbol{\omega} = (\boldsymbol{\imath}, \boldsymbol{\jmath}, \boldsymbol{k})\omega$ is the angular velocity of the body-fixed frame w.r.t. the inertial frame.
- $\boldsymbol{p}, \boldsymbol{v}$ and $\boldsymbol{a}$ denote the CoM's position, translational velocity and acceleration w.r.t. the inertial frame, respectively. Similar notation is also used with the subscript "r" (i.e. $\boldsymbol{p}_r$, $\boldsymbol{v}_r$ and $\boldsymbol{a}_r$) to denote reference trajectories.
- $\tilde{\boldsymbol{p}} = (\boldsymbol{\imath_0}, \boldsymbol{\jmath_0}, \boldsymbol{k_0})\tilde{p} := \boldsymbol{p} - \boldsymbol{p}_r$ and $\tilde{\boldsymbol{v}} = (\boldsymbol{\imath_0}, \boldsymbol{\jmath_0}, \boldsymbol{k_0})\tilde{v} := \boldsymbol{v} - \boldsymbol{v}_r$ denote the position and velocity tracking errors.
- m denotes the vehicle's mass, $\boldsymbol{g}$ the gravitational acceleration, and $\boldsymbol{F}^a$ the resultant of aerodynamic forces acting on the vehicle.
- Either $\dot{\boldsymbol{\xi}}$ or $\frac{d}{dt}\boldsymbol{\xi}_{|\mathcal{I}}$ is used for the time-derivative of $\boldsymbol{\xi} \in \boldsymbol{E}^3$ relatively to the inertial frame.

2.2. Modeling simplifications and motion equations

The actuation inputs used to control the vehicle consist of (i) a propulsion thrust $\boldsymbol{T}$ whose direction $\boldsymbol{u}$ w.r.t. the vehicle's main body can be tilted, (ii) a torque $\boldsymbol{\Gamma}$, independent of the thrust-tilting actuation, used to modify the body's angular velocity $\boldsymbol{\omega}$ at will, and (iii) torques needed to change the thrust direction. Nominally the resultant thrust force passes through the CoM and thus exerts zero torque. Tilting the thrust direction may create a parasitic torque $\boldsymbol{\Gamma}_T$. The control torque $\boldsymbol{\Gamma}$ has to pre-compensate for this parasitic torque and also ensure that (almost) any desired angular velocity is physically obtained rapidly. This leads to consider the angular velocity $\boldsymbol{\omega}$ as an intermediary control input, with the conceptually important advantage of not having to take into account the specificities of the physical torque actuation at this stage of the control design. This justifies the conceptual "backstepping" assumption. We also assume that the thrust intensity T and the thrust-direction tilting angular velocity $\boldsymbol{\omega}^u_{\mathcal{B}}$ are the other control inputs at our disposal.

The equations characterizing the system's dynamics are

$$m\boldsymbol{a} = m\boldsymbol{g} + \boldsymbol{F}^a - T\boldsymbol{u} \tag{1}$$

$$\frac{d}{dt}\{\boldsymbol{\imath}, \boldsymbol{\jmath}, \boldsymbol{k}\}_{|\mathcal{I}} = \boldsymbol{\omega} \times \{\boldsymbol{\imath}, \boldsymbol{\jmath}, \boldsymbol{k}\} \tag{2}$$

$$\frac{d}{dt}\boldsymbol{u}_{|\mathcal{B}} = \boldsymbol{\omega}^u_{\mathcal{B}} \times \boldsymbol{u} \tag{3}$$

with $\boldsymbol{F}^a$ representing all forces, other than thrust and gravitation, applied to the vehicle's body. This vector is typically dominated by lift and drag aerodynamic forces whose intensities depend on the vehicle's longitudinal velocity (relatively to the air) and on the vehicle's attitude when lift is not negligible. For the sake of simplification, and because the focus of the present paper is not to discuss control design aspects specifically related to the aerodynamic forces acting on the vehicle, we here assume that $\boldsymbol{F}^a$ can be decomposed into the sum of two components as follows

$$\boldsymbol{F}^a = \boldsymbol{F}^a_1 + \boldsymbol{F}^a_2 \tag{4}$$

with $\boldsymbol{F}^a_2 = F^a_2\boldsymbol{u}$ ($F^a_2 \in \mathbb{R}$) and $\boldsymbol{F}^a_1$ a vector which, *ideally*, does not depend on the vehicle's orientation. For instance, in the case of a quadrotor UAV with tilted thrust direction, as considered in the simulation Section 4, $\boldsymbol{F}^a$ involves a body-drag force $\boldsymbol{F}^a_D$ and an induced-drag force $\boldsymbol{F}^a_I$ generated by the airflow circulation around the rotors blades. Expressions of these forces are (Mahony, Kumar, & Corke, 2012; Martin & Salaun, 2010):

$$\boldsymbol{F}^a_D = -c_D|\boldsymbol{v}^a|\boldsymbol{v}^a, \qquad \boldsymbol{F}^a_I = -c_l\sqrt{T}(\boldsymbol{v}^a - (\boldsymbol{v}^a \cdot \boldsymbol{u})\boldsymbol{u})$$

with $\boldsymbol{v}^a := \boldsymbol{v} - \boldsymbol{v}_w$ denoting the apparent air velocity, i.e. the vehicle's velocity minus the ambient air velocity $\boldsymbol{v}_w$, and c_D and c_l two aerodynamic coefficients. Summing up these two forces yields

$$\boldsymbol{F}^a = \underbrace{-c_D|\boldsymbol{v}^a|\boldsymbol{v}^a - c_l\sqrt{T}\boldsymbol{v}^a}_{=:\boldsymbol{F}^a_1} + \underbrace{c_l\sqrt{T}(\boldsymbol{v}^a \cdot \boldsymbol{u})\boldsymbol{u}}_{=:\boldsymbol{F}^a_2}.$$

The direction of the drag component $\boldsymbol{F}^a_1$ is, by definition, aligned with the air velocity so that it does not depend on the vehicle's orientation. However, its amplitude depends on this orientation in the general case where the coefficients c_D and $c_l\sqrt{T}$ themselves vary with the vehicle's orientation. Nevertheless, there are flight domains where these coefficients can be considered as almost

constant. For instance, in the absence of wind, for small vehicle's translational velocities the drag force is dominated by the air-velocity linearly dependent term $-c_l\sqrt{T}\boldsymbol{v}^a$. Then, provided that the vehicle's translational acceleration intensity stays smaller than a certain threshold, the thrust T essentially compensates for the vehicle's weight mg so that the drag force can, in this domain, be approximated by the orientation independent term $-c_l\sqrt{mg}\boldsymbol{v}^a$. For the simulations of Section 4, this approximation is made at the control design level, whereas the "true" drag term $-c_l\sqrt{T}\boldsymbol{v}^a$, with the control thrust T depending on the vehicle's orientation, is used to calculate the vehicle's motion.

In view of (4), Eq. (1) can be rewritten as

$$m\boldsymbol{a} = m\boldsymbol{g} + \boldsymbol{F}_1^a - \bar{T}\boldsymbol{u} \tag{5}$$

$$\text{with} \quad \bar{T} := T - F_2^a \tag{6}$$

and an external force $\boldsymbol{F}_1^a$ which – in a certain flight domain and in the first approximation, as explained previously – does not depend on the vehicle's orientation.

3. Control design

We have previously justified the use of $\bar{T}$, defined by (6), $\boldsymbol{\omega}$ and $\boldsymbol{\omega}_{\mathcal{B}}^u$ as control inputs. This section aims at working out feedback control expressions for these inputs.

3.1. Primary objective realization

Using the well-known relations

$$\frac{d}{dt}\boldsymbol{x}_{|\mathcal{I}} = \frac{d}{dt}\boldsymbol{x}_{|\mathcal{B}} + \boldsymbol{\omega}\times\boldsymbol{x}$$
$$\boldsymbol{x}\times(\boldsymbol{y}\times\boldsymbol{z}) = (\boldsymbol{x}\cdot\boldsymbol{z})\boldsymbol{y} - (\boldsymbol{x}\cdot\boldsymbol{y})\boldsymbol{z}$$

for any triplet $(\boldsymbol{x},\boldsymbol{y},\boldsymbol{z}) \in \boldsymbol{E}^3$, and using the definitions of $\boldsymbol{\omega}$, $\boldsymbol{\omega}_{\mathcal{I}}^u$, and $\boldsymbol{\omega}_{\mathcal{B}}^u$, it is simple to show that

$$\frac{d}{dt}\boldsymbol{u}_{|\mathcal{I}} = \boldsymbol{\omega}_{\mathcal{I}}^u\times\boldsymbol{u} \tag{7}$$

$$\boldsymbol{\omega}_{\mathcal{I}}^u = \boldsymbol{\omega}_{\mathcal{B}}^u + \boldsymbol{\omega} - (\boldsymbol{\omega}\cdot\boldsymbol{u})\boldsymbol{u}. \tag{8}$$

Typically $\bar{T}$ and $\boldsymbol{\omega}_{\mathcal{I}}^u$ are determined to achieve a primary objective related to the vehicle's longitudinal motion.

One deduces from (5) the velocity error equation:

$$m\dot{\tilde{\boldsymbol{v}}} = m(\boldsymbol{a}-\boldsymbol{a}_r) = -\bar{T}\boldsymbol{u} + \boldsymbol{F} \tag{9}$$

$$\text{with} \quad \boldsymbol{F} := m\boldsymbol{g} + \boldsymbol{F}_1^a - m\boldsymbol{a}_r. \tag{10}$$

Define $(\tilde{\boldsymbol{\rho}},\tilde{\boldsymbol{v}})$ as a "generalized" error vector. The precise definition of $\tilde{\boldsymbol{\rho}}$ depends on the primary control objective. It can be equal to $\tilde{\boldsymbol{p}}$, if the objective is reference position tracking, or it can be an integral of the velocity error $\tilde{\boldsymbol{v}}$, if the control objective is reference velocity tracking and an integral correction term is needed to improve the control performance. In the case of reference position tracking, it may also be useful to introduce an integral correction. Then, $\tilde{\boldsymbol{\rho}} = (\boldsymbol{I}_p,\tilde{\boldsymbol{p}})$, with $\boldsymbol{I}_p$ denoting a saturated integral of the position tracking error. The simplest case corresponds to pure velocity control without integral correction, for which $\tilde{\boldsymbol{\rho}} = \emptyset$.

Define $\boldsymbol{\xi}(\tilde{\boldsymbol{\rho}},\tilde{\boldsymbol{v}})$ as an intermediary feedback control input that ensures the global asymptotic stability (GAS) and local exponential stability (LES) of the origin $(\tilde{\boldsymbol{\rho}},\tilde{\boldsymbol{v}}) = (\boldsymbol{0},\boldsymbol{0})$ of the nominal system:

$$\dot{\tilde{\boldsymbol{\rho}}} = \boldsymbol{f}(\tilde{\boldsymbol{\rho}},\tilde{\boldsymbol{v}}) \tag{11a}$$

$$\dot{\tilde{\boldsymbol{v}}} = \boldsymbol{\xi}(\tilde{\boldsymbol{\rho}},\tilde{\boldsymbol{v}}). \tag{11b}$$

An example of a function $\boldsymbol{\xi}(\tilde{\boldsymbol{\rho}},\tilde{\boldsymbol{v}})$ is given hereafter in Remark 2. Now, define

$$\boldsymbol{F}_\xi := \boldsymbol{F} - m\boldsymbol{\xi}(\tilde{\boldsymbol{\rho}},\tilde{\boldsymbol{v}}). \tag{12}$$

Then, in view of (9), relation (11b) can be satisfied iff $\bar{T}\boldsymbol{u} = \boldsymbol{F}_\xi$. The following proposition provides a "generalized" result for the control approach proposed in Hua et al. (2009, 2013).

Proposition 1. *Assume that the force $\boldsymbol{F}$ of relation (10) does not vanish along the reference trajectory $\boldsymbol{v}_r$ (i.e., $\exists\delta > 0 : \delta \le |\boldsymbol{F}(\boldsymbol{v}_r^a(t), \boldsymbol{a}_r(t))|,\ \forall t$, with $\boldsymbol{v}_r^a := \boldsymbol{v}_r - \boldsymbol{v}_w$). Define $(\bar{T}_r,\boldsymbol{u}_r) := \left(|\boldsymbol{F}_\xi|,\ \boldsymbol{F}_\xi/|\boldsymbol{F}_\xi|\right)$ and apply to the system (11a)–(9)–(7) the control law:*

$$\bar{T} = \bar{T}_r \quad (\text{or } \bar{T} = \bar{T}_r\boldsymbol{u}\cdot\boldsymbol{u}_r) \tag{13a}$$

$$\boldsymbol{\omega}_{\mathcal{I}}^u = \left(\kappa(\boldsymbol{u},t) + \frac{\dot{\gamma}}{\gamma}\right)\boldsymbol{u}\times\boldsymbol{u}_r + (\boldsymbol{\omega}_{\mathcal{I}}^{u_r} - (\boldsymbol{\omega}_{\mathcal{I}}^{u_r}\cdot\boldsymbol{u})\boldsymbol{u}) \tag{13b}$$

with $\boldsymbol{\omega}_{\mathcal{I}}^{u_r} := \boldsymbol{u}_r\times\frac{d}{dt}\boldsymbol{u}_{r|\mathcal{I}}$ the instantaneous angular velocity of $\boldsymbol{F}_\xi$, $\gamma := \sqrt{c+|\bar{\boldsymbol{F}}_\xi|^2}$ with c any strictly positive constant, and $\kappa(\cdot)$ any continuous positive real-valued function such that $\inf_{\boldsymbol{u},t}\kappa(\boldsymbol{u},t) > 0$.

Then, the equilibrium $(\tilde{\boldsymbol{\rho}},\tilde{\boldsymbol{v}},\boldsymbol{u}) = (\boldsymbol{0},\boldsymbol{0},\boldsymbol{u}_r)$ is locally asymptotically stable. Moreover, all closed-loop solutions such that $\boldsymbol{u} \ne -\boldsymbol{u}_r$ initially and along which $\boldsymbol{F}_\xi$ does not vanish (i.e., $|\boldsymbol{F}_\xi(t)| \ge \delta_\xi > 0,\ \forall t$) converge to $(\boldsymbol{0},\boldsymbol{0},\boldsymbol{u}_r)$.

The proof is the same as the proofs of Propositions 4 and 5 in Pucci, Hamel, Morin, and Samson (2014) complemented with Proposition 1 in Arcak, Angeli, and Sontag (2002), which establishes that the origin of System (11) remains GAS when this system is perturbed by an additive term that is exponentially vanishing and uniformly bounded w.r.t. initial conditions.

Remark 1. The assumption in Proposition 1 is required for the desired thrust direction $\boldsymbol{u}_r$ to be well defined along the reference trajectory. It also guarantees the controllability of the linearized error system and the existence of conventional, either linear or nonlinear, control solutions (Hua et al., 2009, 2013). However, it does not guarantee non-zero crossing of $\boldsymbol{F}_\xi$ for all initial conditions and hence it does not ensure that $\boldsymbol{u}_r$ is always well defined. This also explains why only local stability is established. Preventing $\boldsymbol{F}_\xi$ from crossing zero depends on the nature of the aerodynamic term $\boldsymbol{F}_1^a$. For instance, if $\boldsymbol{F}_1^a \equiv 0$, as often assumed in the literature addressing the hovering case, it suffices to ensure that $|\boldsymbol{\xi}(\tilde{\boldsymbol{\rho}},\tilde{\boldsymbol{v}})| < \min(|\boldsymbol{g}-\boldsymbol{a}_r|)$. In this case almost-global stability can be stated. The reader is invited to consult (Hua et al., 2009) for possible ways to modify the control law when $\boldsymbol{F}_\xi$ gets near zero and also for control regularization when this term temporarily vanishes.

Remark 2. Proposition 1 provides a unifying control design framework for different primary objectives. Consider, for instance, the problem of tracking a reference position trajectory with a controller including a saturated integral $\boldsymbol{I}_p$ of the position error, in order to compensate for static modeling errors. An example of such an integral term is obtained as the (numerical) solution to the following equation (Hua & Samson, 2011):

$$\begin{cases} \boldsymbol{I}_p = (\boldsymbol{\imath}_{\boldsymbol{0}},\boldsymbol{\jmath}_{\boldsymbol{0}},\boldsymbol{k}_{\boldsymbol{0}})I_p \\ \ddot{I}_p = -k_{dI}\dot{I}_p + \sigma^{\frac{\ddot{I}_{p,\max}}{2}}\left(k_{pI}\left(-I_p + \sigma^{\Delta_{I_p}}\left(I_p + \frac{\tilde{p}}{k_{pI}}\right)\right)\right) \end{cases} \tag{14}$$

with zero initial conditions, i.e. $I_p(0) = \dot{I}_p(0) = 0$, positive numbers k_{pI}, k_{dI}, $\ddot{I}_{p,\max}$ and Δ_{I_p}, and $\sigma^\Delta(x) \in \mathbb{R}^3,\ \forall x \in \mathbb{R}^3$ denoting a twice-differentiable approximation function of the classical saturation function $\text{sat}^\Delta(x) := \min(1,\Delta/|x|)x$. Then, $\tilde{\boldsymbol{\rho}} = (\dot{\boldsymbol{I}}_{\boldsymbol{p}},\boldsymbol{I}_p,\tilde{\boldsymbol{p}})$. An exponential stabilizer of the origin of System (11) is the following nonlinear "PID" controller, used for simulations in Section 4:

$$\boldsymbol{\xi}(\tilde{\boldsymbol{\rho}},\tilde{\boldsymbol{v}}) = (\boldsymbol{\imath}_{\boldsymbol{0}},\boldsymbol{\jmath}_{\boldsymbol{0}},\boldsymbol{k}_{\boldsymbol{0}})\big(-k_p\sigma^{\Delta_p}(\tilde{p}+k_iI_p) - k_d\sigma^{\Delta_v}(\tilde{v}+k_i\dot{I}_p) - k_i\ddot{I}_p\big) \tag{15}$$

with $k_p, k_i, k_d, \Delta_p, \Delta_v$ positive constants. Indeed, applying this controller to System (11) yields

$$\ddot{\bar{p}} + k_d \sigma^{\Delta_v}(\dot{\bar{p}}) + k_p \sigma^{\Delta_p}(\bar{p}) = 0; \quad \bar{p} := \tilde{p} + k_i I_p.$$

Using the Lyapunov function $\mathcal{V}(\bar{p}, \dot{\bar{p}}) := \frac{1}{2}|\dot{\bar{p}}|^2 + k_p \int_0^{|\bar{p}|} h(s)ds$, where the function $h(\cdot) \in \mathbb{R}$ satisfies $h(|x|)\frac{x}{|x|} = \sigma^{\Delta_p}(x), \forall x \in \mathbb{R}^3$, and the time-derivative of $\mathcal{V}$ verifies $\dot{\mathcal{V}} = -k_d \dot{\bar{p}} \cdot \sigma^{\Delta_v}(\dot{\bar{p}}) \leq 0$, one shows that the origin of this system is LES and GAS. Finally, one shows that the convergence of $(\bar{p}, \dot{\bar{p}})$ to zero also ensures the convergence of $(\tilde{p}, \tilde{v})$ to zero (see, e.g., Hua et al., 2009 and Hua & Samson, 2011 for details).

3.2. Secondary objective realization

The thrust intensity T (or equivalently $\bar{T}$ via (6)) has been determined previously. It remains to determine $\boldsymbol{\omega}$ and $\boldsymbol{\omega}^u_{\mathcal{B}}$ that satisfy (8) with $\boldsymbol{\omega}^u_{\mathcal{I}}$ given by (13b), as imposed by the realization of the primary objective, and also allow for the realization of a secondary objective.

Let $\boldsymbol{\omega}^\star$ denote the angular velocity control that would be used for the secondary control objective if the thrust-tilting angle was not limited. For instance, this objective can be the asymptotic stabilization of the body-fixed frame vector $\boldsymbol{k}$ at a reference time-varying unit vector $\boldsymbol{k}_r$. Then, a possible control, whose expression is obtained in the same way as the control $\boldsymbol{\omega}^u_{\mathcal{I}}$ in (13b) by rendering the time-derivative of the Lyapunov function candidate $\frac{1-\boldsymbol{k}\cdot\boldsymbol{k}_r}{1+\boldsymbol{k}\cdot\boldsymbol{k}_r}$ negative when $\boldsymbol{k} \neq \boldsymbol{k}_r$, is

$$\boldsymbol{\omega}^\star = \boldsymbol{\omega}^{k_r}_{\mathcal{I}} + \kappa_\omega \boldsymbol{k} \times \boldsymbol{k}_r + \lambda \boldsymbol{k} \tag{16}$$

with $\boldsymbol{\omega}^{k_r}_{\mathcal{I}} := \boldsymbol{k}_r \times \frac{d}{dt}\boldsymbol{k}_{r|\mathcal{I}}$ the instantaneous angular velocity of $\boldsymbol{k}_r$ w.r.t. the inertial frame, $\kappa_\omega > 0$, and $\lambda \in \mathbb{R}$ any real-valued function. The indetermination of λ corresponds to the unused d.o.f associated with rotations about the $\boldsymbol{k}$ direction. If the secondary objective is to asymptotically stabilize a reference orientation for the vehicle's body, then a possible control is

$$\boldsymbol{\omega}^\star = \boldsymbol{\omega}_r - \kappa_\omega \tan(\theta/2)\boldsymbol{v}; \quad \kappa_\omega > 0 \tag{17}$$

with $\theta\boldsymbol{v}$ the rotation vector associated with the orientation error between the body-fixed frame and the reference orientation, and $\boldsymbol{\omega}_r$ the reference angular velocity associated with the reference orientation.

Let us define

$$\boldsymbol{\omega}^{u\,\star}_{\mathcal{B}} := \boldsymbol{\omega}^u_{\mathcal{I}} - (\boldsymbol{\omega}^\star - (\boldsymbol{\omega}^\star \cdot \boldsymbol{u})\boldsymbol{u}). \tag{18}$$

Since $\boldsymbol{\omega}^{u\,\star}_{\mathcal{B}}$ satisfies (8) when $\boldsymbol{\omega}$ is equal to the unconstrained solution $\boldsymbol{\omega}^\star$, it is the thrust-tilting angular velocity that would be used in the unconstrained case to achieve both primary and secondary objectives. However, due to the thrust-tilting angle limitation, modified expressions for $\boldsymbol{\omega}$ and $\boldsymbol{\omega}^u_{\mathcal{B}}$ have to be worked out. To this aim, let us first specify the maximum value of the thrust-tilting angle and set

$$\delta = \max\left(\sqrt{u_1^2 + u_2^2}\right) \quad (< 1) \tag{19}$$

so that the maximum tilting angle is $\arcsin(\delta) \in [0, \frac{\pi}{2})$.

Define

$$\boldsymbol{\mu} := \boldsymbol{\omega}^{u\,\star}_{\mathcal{B}} \times \boldsymbol{u} \tag{20}$$

and denote μ as the vector of coordinates of $\boldsymbol{\mu}$ on the basis of the body-fixed frame, i.e. $\boldsymbol{\mu} = \{\boldsymbol{\imath}, \boldsymbol{\jmath}, \boldsymbol{k}\}\mu$. The tilting angle is modified according to the following control law:

$$\dot{u}_{1,2} = -k_u u_{1,2} + k_u \mathrm{sat}^\delta(u_{1,2} + \mu_{1,2}/k_u) \tag{21}$$

with initial conditions satisfying $|u_{1,2}(0)| \leq \delta$, k_u a positive number (not necessarily constant).

Theorem 1. *Apply to the system (11a)–(9)–(2)–(3) the control law*

$$\bar{T} = \bar{T}_r \quad (\text{or } \bar{T} = \bar{T}_r \boldsymbol{u} \cdot \boldsymbol{u}_r) \tag{22a}$$

$$\boldsymbol{\omega}^u_{\mathcal{B}} = \boldsymbol{u} \times \frac{d}{dt}\boldsymbol{u}_{|\mathcal{B}} \tag{22b}$$

$$\boldsymbol{\omega} = \boldsymbol{\omega}^u_{\mathcal{I}} - \boldsymbol{\omega}^u_{\mathcal{B}} + (\boldsymbol{\omega}^\star \cdot \boldsymbol{u})\boldsymbol{u} \tag{22c}$$

with $\boldsymbol{\omega}^u_{\mathcal{I}}$ given by (13b), $\frac{d}{dt}\boldsymbol{u}_{|\mathcal{B}} = \{\boldsymbol{\imath}, \boldsymbol{\jmath}, \boldsymbol{k}\}\dot{u}$, $\dot{u}_{1,2}$ given by (21) and $\dot{u}_3 = -\frac{u_{1,2}^T \dot{u}_{1,2}}{u_3} = -\frac{u_{1,2}^T \dot{u}_{1,2}}{\sqrt{1-u_1^2-u_2^2}}$, using the fact that $\boldsymbol{u}$ is a unit vector.

Then, provided that the assumption in Proposition 1 is satisfied, the following properties hold:

1. *The primary objective is realized, as specified in Proposition 1.*
2. *The thrust-tilting angle remains smaller or equal to the maximum tilting angle, i.e. $|u_{1,2}(t)| \leq \delta$, $\forall t$.*
3. *When $|u_{1,2} + \mu_{1,2}/k_u| \leq \delta$, one has $\boldsymbol{\omega}^u_{\mathcal{B}} = \boldsymbol{\omega}^{u\,\star}_{\mathcal{B}}$ and $\boldsymbol{\omega} = \boldsymbol{\omega}^\star$, which implies the realization of the secondary objective.*

Proof. In view of (21),

$$\begin{aligned}\frac{1}{2}\frac{d}{dt}|u_{1,2}|^2 &= -k_u|u_{1,2}|^2 + k_u u_{1,2}^T \mathrm{sat}^\delta(u_{1,2} + \mu_{1,2}/k_u) \\ &\leq -k_u|u_{1,2}|^2 + k_u\delta|u_{1,2}|\end{aligned}$$

and the latter inequality implies that $|u_{1,2}|$ remains smaller or equal to δ, provided that the initial value of $|u_{1,2}|$ is itself chosen smaller or equal to δ.

One easily verifies from (21) that $\dot{u} = \mu$, i.e. $\frac{d}{dt}\boldsymbol{u}_{|\mathcal{B}} = \boldsymbol{\mu}$, when $|u_{1,2} + \mu_{1,2}/k_u| \leq \delta$, which in turn implies that $\boldsymbol{\omega}^u_{\mathcal{B}} = \boldsymbol{\omega}^{u\,\star}_{\mathcal{B}}$ when $|u_{1,2} + \dot{u}^\star_{1,2}/k_u| \leq \delta$. Then, one deduces from (22c) and the relations $\boldsymbol{u} \cdot \boldsymbol{\omega}^u_{\mathcal{I}} = \boldsymbol{u} \cdot \boldsymbol{\omega}^u_{\mathcal{B}} = \boldsymbol{0}$ that $\boldsymbol{\omega} \cdot \boldsymbol{u} = \boldsymbol{\omega}^\star \cdot \boldsymbol{u}$ and, subsequently, that $\boldsymbol{\omega} = \boldsymbol{\omega}^\star$ when $|u_{1,2} + \mu_{1,2}/k_u| \leq \delta$. Moreover, the equality (8) is always satisfied with this choice, in accordance with the priority given to the realization of the primary objective. ■

Remarks.

- For $u_{1,2}$ to be dominant on the left-hand side of the inequality $|u_{1,2} + \mu_{1,2}/k_u| \leq \delta$ (allowing for the realization of the secondary objective), k_u should be chosen large enough.
- Thrust-tilting may involve only a single rotation about a body-fixed axis (see, e.g., Cetinsoy et al., 2012; Notarstefano & Hauser, 2010; Papachristos et al., 2011; Russo et al., 2011) in contrast with the two d.o.f. rotation case here considered. A straightforward adaptation of the proposed control design for the realization of the secondary objective then consists in replacing the control law (21) by

$$\begin{cases}\dot{u}_1 = -k_u u_1 + k_u \mathrm{sat}^\delta(u_1 + \mu_1/k_u) \\ \dot{u}_2 = u_2 = 0.\end{cases}$$

4. Application to a thrust-tilted quadrotor UAV

The above control solution has been tested on the model of a quadrotor UAV sketched in Fig. 1. We assume that the four rotor axes can be simultaneously tilted and in the same direction corresponding to the overall thrust direction $\boldsymbol{u}$. Let P_i $(i = 1, \ldots, 4)$ be the pivoting points of the four rotors, with their positions in the body frame $\boldsymbol{GP}_1 = h\boldsymbol{k} + d\boldsymbol{\imath}$, $\boldsymbol{GP}_2 = h\boldsymbol{k} - d\boldsymbol{\jmath}$, $\boldsymbol{GP}_3 = h\boldsymbol{k} - d\boldsymbol{\imath}$, $\boldsymbol{GP}_4 = h\boldsymbol{k} + d\boldsymbol{\jmath}$, with $h \in \mathbb{R}$ and $d > 0$. In Fig. 1, $h = 0$.

Let ϖ_i $(i = 1, \ldots, 4)$ denote the angular velocities of the four rotors. According to Hamel, Mahony, Lozano, and Ostrowski (2002), the ith rotor generates a thrust force $\boldsymbol{T}_i = -\alpha\varpi_i^2\boldsymbol{u}$ and a drag torque $\boldsymbol{Q}_i = \lambda_i\beta\varpi_i^2\boldsymbol{u}$, with α and β two aerodynamic coefficients and $\lambda_i = 1$ (resp. -1) if i is odd (resp. even). The thrust $\boldsymbol{T}$ and the torque vector $\boldsymbol{\Gamma} = (\boldsymbol{\imath}, \boldsymbol{\jmath}, \boldsymbol{k})\Gamma$ generated by the four rotors

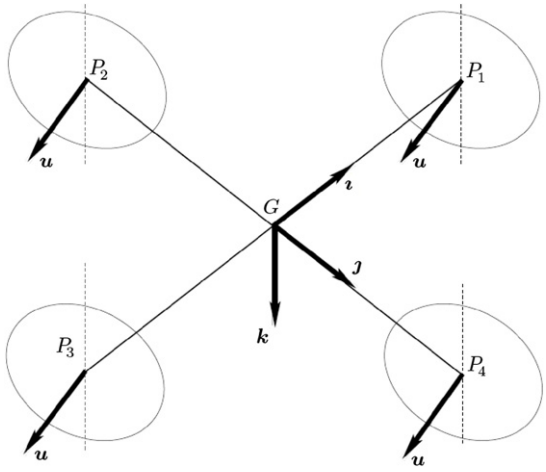

Fig. 1. Sketch of a quadrotor with thrust-tilting capability.

are given by

$$\begin{aligned}\boldsymbol{T} &= \sum_i \boldsymbol{T}_i = \alpha\left(\sum_i \varpi_i^2\right)\boldsymbol{u}\\ \boldsymbol{\Gamma} &= \sum_i (\boldsymbol{GP}_i \times \boldsymbol{T}_i + \boldsymbol{Q}_i)\\ &= -d\alpha(\varpi_1^2 - \varpi_3^2)(\boldsymbol{\imath}\times\boldsymbol{u}) + d\alpha(\varpi_2^2 - \varpi_4^2)(\boldsymbol{\jmath}\times\boldsymbol{u})\\ &\quad - h\alpha\sum_i \varpi_i^2(\boldsymbol{k}\times\boldsymbol{u}) + \sum_i \lambda_i\beta\varpi_i^2\boldsymbol{u}.\end{aligned}$$

One deduces the following relation between the vector of rotors angular velocities ϖ_i and the vector composed of the thrust intensity and the control torque components:

$$\begin{bmatrix}T & \Gamma\end{bmatrix}^T = A_{mot}\begin{bmatrix}\varpi_1^2 & \varpi_2^2 & \varpi_3^2 & \varpi_4^2\end{bmatrix}^T$$

with the allocation matrix A_{mot} defined by

$$\begin{bmatrix}\alpha & \alpha & \alpha & \alpha\\ h\alpha u_2 + \beta u_1 & a_{22} & h\alpha u_2 + \beta u_1 & a_{24}\\ a_{31} & -h\alpha u_1 - \beta u_2 & a_{33} & -h\alpha u_1 - \beta u_2\\ -d\alpha u_2 + \beta u_3 & -d\alpha u_1 - \beta u_3 & d\alpha u_2 + \beta u_3 & d\alpha u_1 - \beta u_3\end{bmatrix}$$

with $a_{22} := h\alpha u_2 + d\alpha u_3 - \beta u_1$, $a_{24} := h\alpha u_2 - d\alpha u_3 - \beta u_1$, $a_{31} := -h\alpha u_1 + d\alpha u_3 + \beta u_2$, $a_{33} := -h\alpha u_1 - d\alpha u_3 + \beta u_2$. Since A_{mot} is invertible ($\det(A_{mot}) = 8\beta d^2\alpha^3 u_3 > 0$), T and Γ can be given any desired values – modulo the constraint of positivity of the rotors angular velocities and the limited range of velocities imposed by power limitations of the rotors – and can thus be used as independent control variables. The direct application of the proposed control strategy relies on this actuation property.

4.1. Simulation results

Specifications of the simulated vehicle are as follows:

- Mass: $m = 1.5$ (kg),
- Moment of Inertia: $I = \mathrm{diag}(0.028, 0.028, 0.06)$ (kg m^2),
- Level arm values: $[h, d] = [0.05, 0.2]$ (m),
- Thrust angle limitation: $\pi/6$ (rad),
- Body drag coeff. $c_D = 0.0092$ (kg m^{-1}),
- Induced drag coeff. $c_l = 0.0959$ (kg s^{-1}).

Concerning the calculation of the torque Γ in charge of producing the desired body angular velocity defined by (22c), we have used $\Gamma = -k_\omega I(\omega - \omega^\star) + \omega \times I\omega^\star$, with $\omega^\star$ the vector of coordinates, expressed in the body-fixed frame, of the reference angular velocity defined by (22c), and k_ω a positive gain. Due to the parasitic torque induced by the chosen non-zero value of h (one of the parameters characterizing the position of the propellers) and the non pre-compensation of both this torque and the reference angular acceleration $\dot\omega^\star$ in the expression of Γ, there remains a residual error between ω and $\omega^\star$ in the general case. We have made this simplification in the control calculation in order to test the robustness of the proposed control design against (inevitable) modeling errors. This explains residual position tracking errors that are observable in the reported simulation results.

The primary objective considered for these simulations is the position tracking of an eight-shaped Lissajous trajectory defined by: $\boldsymbol{x}_r = 5\sin(a_r t)\boldsymbol{\imath}_0 + 5\sin(2a_r t)\boldsymbol{\jmath}_0$. By changing the parameter a_r, one modifies the time period of a complete run, as well as the associated reference velocity and acceleration. Two values of a_r ($2\pi/15$ and $\pi/5$) are considered. The first one corresponds to a "slow" run (Simulation 1) that involves non-saturated thrust-direction tilt angles, whereas the second one corresponds to a "fast" run (Simulation 2) along portions of which the tilt angle attains its maximum value.

The chosen secondary objective is the stabilization of the vehicle's attitude about the identity matrix. In particular, the realization of this objective requires the vehicle's plane containing the rotors' pivot points $P_{1,2,3,4}$ to remain horizontal all the time. The associated angular velocity control $\boldsymbol{\omega}^\star$ is given by (17).

The control gains and other parameters involved in the calculation of the control inputs are chosen as follows:

- $\kappa(\boldsymbol{u}, t) = 30$, $c = 0.01$,
- $k_p = 1.21$, $k_d = 1.55$, $k_i = 0.24$, $\Delta_p = \frac{4}{k_p}$, $\Delta_v = \frac{4}{k_d}$,
- $k_{dI} = 4$, $k_{pI} = 4$, $\Delta_{I_p} = \frac{4}{k_i}$, $\ddot{I}_{p,\max} = \frac{4}{k_i}$,
- $\kappa_\omega = 10$, $k_u = 20$, $k_\omega = 20$.

In the control expression, the aerodynamic force $\boldsymbol{F}_1^a$ is approximated by $\boldsymbol{F}_1^a \approx -c_D|\boldsymbol{v}_r|\boldsymbol{v}_r - c_l\sqrt{mg}\boldsymbol{v}_r$ which is obtained by replacing T and $\boldsymbol{v}^a$ by mg and $\boldsymbol{v}_r$, respectively. The time-derivative of this force, also needed for the control calculation, is calculated accordingly. Initial conditions for the vehicle's configuration are as follows:

$$\begin{cases}\boldsymbol{x}(0) = 0.8\boldsymbol{\jmath}_0, & \boldsymbol{v}(0) = 5a_r\boldsymbol{\imath}_0 + 10a_r\boldsymbol{\jmath}_0,\\ \{\boldsymbol{\imath}(0), \boldsymbol{\jmath}(0), \boldsymbol{k}(0)\} = \{\boldsymbol{\imath}_0, \boldsymbol{\jmath}_0, \boldsymbol{k}_0\},\\ \boldsymbol{u}(0) = \boldsymbol{k}(0), & \boldsymbol{\omega}(0) = \boldsymbol{\omega}_{\mathcal{B}}^{u}(0) = \boldsymbol{0}.\end{cases}$$

Two simulations, in the absence of wind (i.e., $\boldsymbol{v}_w = \boldsymbol{0}$), are reported next.

- *Simulation* 1 ($a_r = 2\pi/15$): The time period for a complete run is 15 s. The projection on the horizontal plane of the path followed by the vehicle's CoM is shown in Fig. 2. Variations w.r.t. time of the vehicle and thrust inclination angles, of the position tracking errors, and of the thrust magnitude, are shown in Figs. 3–5. In Figs. 2 and 3 the nine highlighted points correspond to time-instants when the reference trajectory involves large acceleration variations. From Fig. 2 one can observe that the vehicle catches up with, and subsequently closely follows, the reference trajectory. Despite a rather aggressive reference trajectory, with an average longitudinal velocity of about 4 m/s and accelerations sometimes exceeding 3 m/s^2, the vehicle's base remains always horizontal (see Fig. 3). One can also observe from Fig. 3 that the thrust-direction tilt angle never reaches its maximum value (equal to $\pi/6$ rad). Both goals are thus achieved (almost) perfectly in this case.
- *Simulation* 2 ($a_r = \pi/5$): This simulation is devised to illustrate the effects of thrust-tilting saturation and the corresponding control monitoring. The time-period for a complete run is reduced to 10 s and the reference trajectory is more aggressive than the one in Simulation 1. Results are shown in Figs. 6–10. One can now observe from Fig. 7 that the vehicle's inclination periodically departs from zero when the thrust-direction tilt

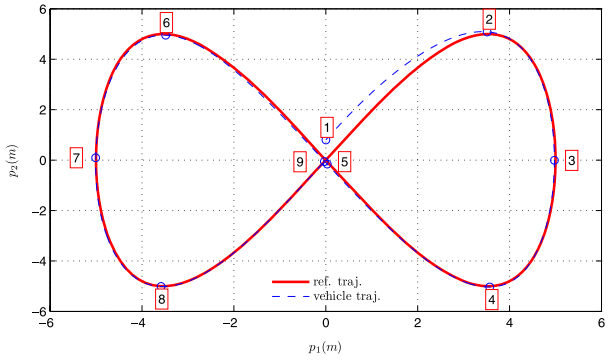

Fig. 2. Reference and vehicle trajectories projected on the horizontal plane (Sim. 1).

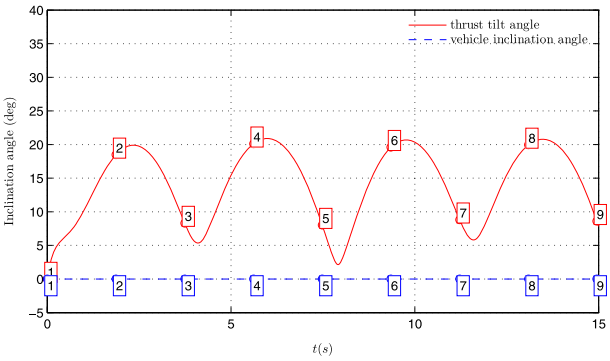

Fig. 3. Thrust and vehicle inclination angles vs. time (Sim. 1).

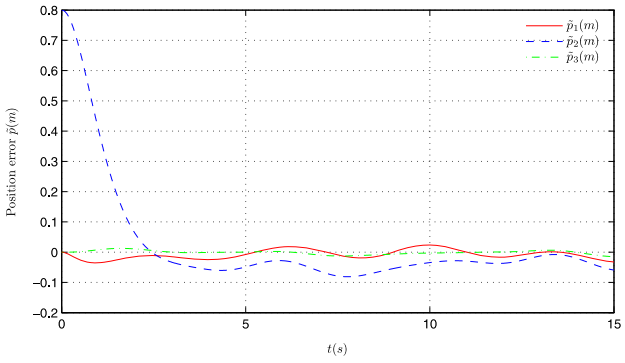

Fig. 4. Position tracking errors vs. time (Sim. 1).

angle attains its maximum value. While the primary position tracking task is again performed perfectly, the secondary objective is, as expected, imperfectly realized in this case. However, the body's inclination returns to the desired zero value as soon as the thrust tilt angle needed to achieve the secondary objective re-enters the domain of allowed tilt angles, a behavior that we find satisfactory. Finally, a video showing the simulations results is available at http://youtu.be/e7nreUHVbbk.

5. Conclusion

Nonlinear control of VTOL vehicles endowed with thrust-tilting capability has been addressed and a generic control solution exploiting thrust-tilting augmentation has been devised. The proposed solution potentially applies to a large panel of aerial vehicles with extended flight envelopes. It involves a primary objective consisting in the asymptotic stabilization of either a reference velocity or a reference position trajectory, and a secondary

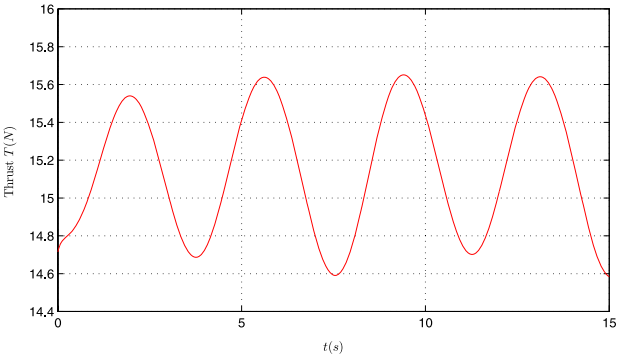

Fig. 5. Thrust intensity vs. time (Sim. 1).

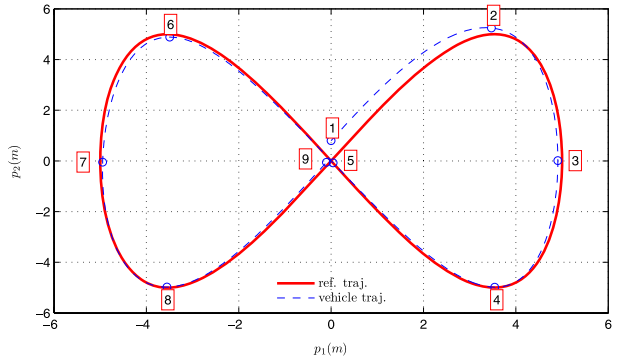

Fig. 6. Reference and vehicle trajectories projected on the horizontal plane (Sim. 2).

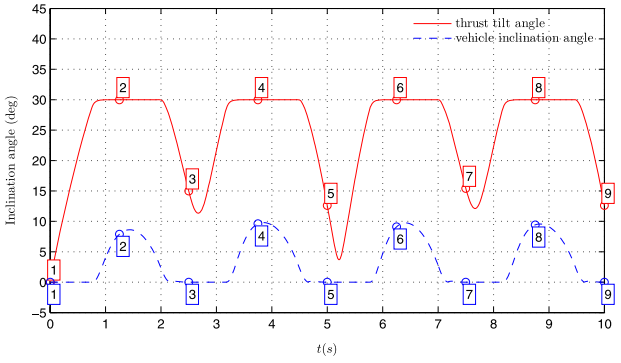

Fig. 7. Thrust and vehicle inclination angles vs. time (Sim. 2).

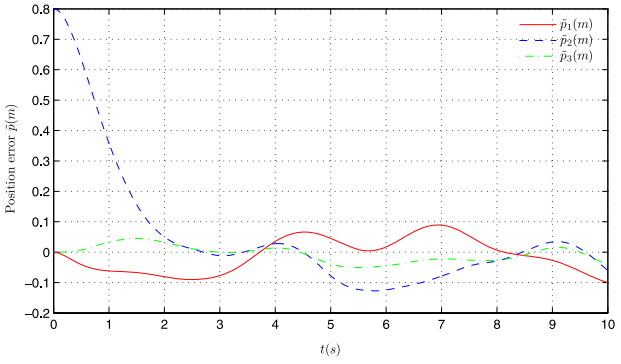

Fig. 8. Position tracking errors vs. time (Sim. 2).

objective consisting in the asymptotic stabilization of either a reference direction for one of the body-base vectors or a complete reference orientation for the body-fixed frame. A major original outcome of the present study is the definition of a control solution

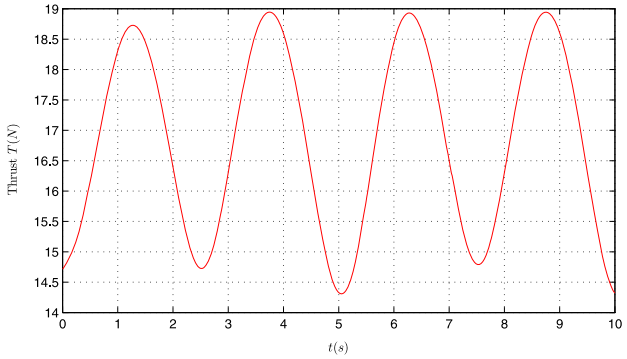

Fig. 9. Thrust intensity vs. time (Sim. 2).

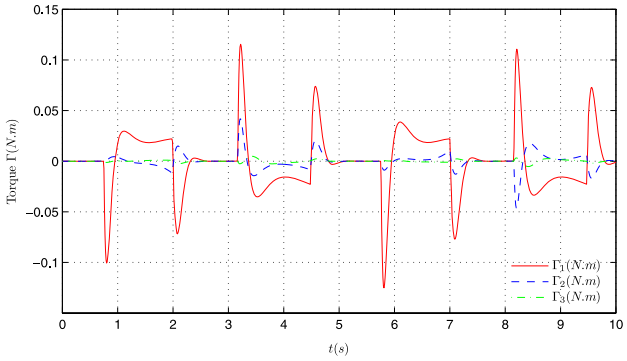

Fig. 10. Torque inputs vs. time (Sim. 2).

that takes thrust-tilting limitations into account explicitly. We view it also as new contribution to the ongoing development of a unified nonlinear approach to the control of aerial vehicles, in the continuation of Hua et al. (2009); Hua, Pucci, Hamel, Morin, and Samson (in press), Pucci (2011) and Pucci et al. (2014). Many open problems on this topic remain. Perspectives include the extension of the proposed approach in order to properly account for the dependence of the aerodynamic forces on the vehicle's orientation, as in the case of twin tilt-rotors and tilt-wing UAVs. In addition, since the proposed thrust-tilting control strategy has been so far validated only in simulation, experiments carried out on physical devices are thus needed to adapt the approach to the specificities of each flying device and assert its practical usefulness.

References

Arcak, M., Angeli, D., & Sontag, E. (2002). A unifying integral ISS framework for stability of nonlinear cascades. *SIAM Journal on Control and Optimization*, *40*(6), 1888–1904.

Cetinsoy, E., Dikyar, S., Hancer, C., Oner, K. T., Sirimoglu, E., Unel, M., et al. (2012). Design and construction of a novel quad tilt-wing UAV. *Mechatronics*, *22*(6), 723–745.

Hamel, T., Mahony, R., Lozano, R., & Ostrowski, J. (2002). Dynamic modelling and configuration stabilization for an X4-flyer. In *IFAC world congress* (pp. 200–212).

Hua, M.-D., Hamel, T., Morin, P., & Samson, C. (2009). A control approach for thrust-propelled underactuated vehicles and its application to VTOL drones. *IEEE Transactions on Automatic Control*, *54*(8), 1837–1853.

Hua, M.-D., Hamel, T., Morin, P., & Samson, C. (2013). Introduction to feedback control of underactuated VTOL vehicles. *IEEE Control Systems Magazine*, *33*(1), 61–75.

Hua, M.-D., Hamel, T., Morin, P., & Samson, C. (2014). Control of VTOL vehicles with thrust-tilting augmentation. In *IFAC world congress* (pp. 2237–2244).

Hua, M.-D., Pucci, D., Hamel, T., Morin, P., & Samson, C. (2014). A novel approach to the automatic control of scale model airplanes. In *IEEE conf. on decision and control* (in press).

Hua, M.-D., & Samson, C. (2011). Time sub-optimal nonlinear PI and PID controllers applied to longitudinal headway car control. *International Journal of Control*, (10), 1717–1728.

Kendoul, F., Fantoni, I., & Lozano, R. (2005). Modeling and control of a small autonomous aircraft having two tilting rotors. In *IEEE conf. on decision and control* (pp. 8144–8149).

Long, Y., & Cappelleri, D.J. (2013). Complete dynamic modeling, control and optimization for an over-actuated MAV. In *IEEE/RSJ int. conf. on intelligent robots and systems* (pp. 1380–1385).

Mahony, R., Kumar, V., & Corke, P. (2012). Multirotor aerial vehicles: modeling, estimation, and control of quadrotor. *IEEE Robotics & Automation Magazine*, *19*(3), 20–32.

Martin, P., & Salaun, E. (2010). The true role of accelerometer feedback in quadrotor control. In *IEEE int. conf. on robotics and automation* (pp. 1623–1629).

Muraoka, K., Okada, N., & Kubo, D. (2009). Quad tilt wing VTOL UAV: aerodynamic characteristics and prototype flight test. In *AIAA Infotech@ aerospace conf., Number 1834*.

Naldi, R., Marconi, L., & Sala, A. (2008). Modelling and control of a miniature ducted-fan in fast forward flight. In *American control conf.* (pp. 2552–2557).

Notarstefano, G., & Hauser, J. (2010). Modeling and dynamics exploration of a tilt-rotor VTOL aircraft. In *IFAC symp. on nonlinear control systems* (pp. 119–124).

Papachristos, C., Alexis, K., & Tzes, A. (2011). Design and experimental attitude control of an unmanned tilt-rotor aerial vehicle. In *IEEE int. conf. on advanced robotics* (pp. 465–470).

Pflimlin, J.-M., Binetti, P., Souères, P., Hamel, T., & Trouchet, D. (2010). Modeling and attitude control analysis of a ducted-fan micro aerial vehicle. *Control Engineering Practice*, 209–218.

Pucci, P. (2011). Flight dynamics and control in relation to stall. In *American control conf.* (pp. 118–124).

Pucci, D., Hamel, T., Morin, P., & Samson, C. (2014). Nonlinear feedback control of axisymmetric aerial vehicles. ArXiv Preprint arXiv:1403:5290.

Russo, E., Notarstefano, G., & Hauser, J. (2011). Dynamics exploration and aggressive maneuvering of a longitudinal vectored thrust VTOL aircraft. In *IEEE conf. on decision and control* (pp. 119–124).

Ryll, M., Bulthoff, H.H., & Giordano, P.R. (2012). Modeling and control of a quadrotor UAV with tilting propellers. In *IEEE int. conf. on robotics and automation* (pp. 4606–4613).

Minh-Duc Hua graduated from Ecole Polytechnique in 2006, and received his Ph.D. degree from the University of Nice Sophia Antipolis in 2009. He spent two years as a post-doctoral fellow at the laboratory I3S UNS-CNRS, France. He is currently Chargé de Recherche of the French National Center for Scientific Research (CNRS) and has been working at the Institute for Intelligent Systems and Robotics (ISIR UPMC-CNRS) in Paris since 2011. His research interests include nonlinear control, sensor-based control and nonlinear observer with applications to UAVs and AUVs.

Tarek Hamel is a Professor at the University of Nice Sophia Antipolis since 2003. He received his Ph.D. degree in Robotics from the University of Technology of Compiègne (UTC), France, in 1996. After two years as a research assistant at the UTC, he joined the Centre d'Etudes de Mécanique d'Ile de France in 1997 as an associate professor. His research interests include nonlinear control theory, estimation and vision-based control with applications to Unmanned Aerial Vehicles. He is currently an Associate Editor for IEEE Transactions on Robotics and for Control Engineering Practice.

Pascal Morin received the Diplôme d'Ingénieur and Ph.D. degrees from Ecole des Mines de Paris in 1992 and 1996 respectively. He spent one year as a post-doctoral fellow in the Control and Dynamical Systems Department at the California Institute of Technology. He was Chargé de Recherche at INRIA from 1997 to 2011. He is currently in charge of the "Chaire RTE-UPMC Mini-drones autonomes" at the ISIR lab of University Pierre and Marie Curie (UPMC) in Paris. His research interests include stabilization and estimation problems for nonlinear systems, and applications to mechanical systems such as nonholonomic vehicles or UAVs.

Claude Samson graduated from the Ecole Supérieure d'Electricité in 1977, and received his Docteur-Ingénieur and Docteur d'Etat degrees from the University of Rennes, in 1980 and 1983, respectively. He joined INRIA in 1981, where he is presently Directeur de Recherche. His research interests are in control theory and its applications to the control of mechanical systems. Dr. Samson is the coauthor, with M. Leborgne and B. Espiau, of the book *Robot Control. The Task-Function Approach* (Oxford University Press, 1991).